Recent thinning and migration of the Western Divide, central West Antarctica

H. Conway[1] and L. A. Rasmussen[1]

Received 6 March 2009; revised 5 May 2009; accepted 22 May 2009; published 23 June 2009.

[1] We report observations that show the Western Divide, between the Ross and Amundsen Sea sectors in West Antarctica, is currently thinning ~0.08 m a^{-1} and migrating toward the Ross Sea at 10 m a^{-1}. The asymmetric pattern of thickness change across the divide is not caused by changes in the accumulation gradient, but rather by dynamical thinning that is stronger in the Amundsen Sea sector than in the Ross Sea sector. Available geological and glaciological data indicate that this pattern of thinning has persisted for at least two millennia, with increased asymmetry likely over the past few centuries. Our data however, are not sufficient to determine whether the present-day migration of the Western Divide is a response to long-term (millennial) forcing, shorter-term (centennial) forcing, or both. **Citation:** Conway, H., and L. A. Rasmussen (2009), Recent thinning and migration of the Western Divide, central West Antarctica, *Geophys. Res. Lett.*, *36*, L12502, doi:10.1029/2009GL038072.

1. Introduction

[2] Changes in activity of fast-flowing outlet glaciers and ice streams exert strong control on the mass balance of the West Antarctic Ice Sheet; mass change of the Ross Sea sector has been positive since Kamb Ice Stream stagnated about 180 years ago [*Joughin and Tulaczyk*, 2002], while increased flow speeds of Pine Island and Thwaites Glaciers over the past few decades have resulted in large mass losses from the Amundsen Sea sector [*Rignot et al.*, 2008]. Observations from Pine Island Glacier show strong coupling between coastal regions and the upper reaches. Specifically, velocity perturbations at the grounding line propagated rapidly (less than two decades) more than 100-km upstream [*Shepherd et al.*, 2004]. Ice-flow models reproduce this tight coupling and fast response [e.g., *Joughin et al.*, 2009; *Payne et al.*, 2004; *Alley et al.*, 1987]. A fundamental question relevant to the future stability of the West Antarctic Ice Sheet is therefore: Can the onset regions of fast-flowing glaciers and ice streams migrate inland? If so, how far can they migrate, and how fast? Large length-scales or short time-scales have important implications for sea level rise. Length-scales all the way from the coast to the ice divide imply that the reservoir available for discharge is large. Short time-scales imply that it could be sudden.

2. Field Measurements

[3] Here we investigate ice flow at the Western Divide, which separates the Ross and Amundsen Sea sectors of West Antarctica (Figure 1). We analyze measurements made by us during austral summers of 2002–2003 and 2003–2004 as part of the site selection for the WAIS divide core (WDC). Measurements include repeat surveys (13 months apart) of a network of 98 poles (Figure 2) using the Global Positioning System (GPS). Measurements were used to map the surface topography (Figure 2a) and to calculate the surface velocity field (Figure 2b). Mean uncertainty in the velocity components calculated over the 1.1-year interval is 0.04 m a^{-1}. Ice-penetrating radar profiles along and between the three primary pole lines (Figures 1 and 2a) were used to map both ice thickness and internal layers. Uncertainty in depth of a reflecting layer arises primarily from uncertainty in the wave speed in ice (about ±2 m μs^{-1}, which corresponds to ~1.2% of the depth to the reflector), and from ambiguity in picking the two-way travel time (±0.01 μs or about ±1 m in ice); uncertainty is about 42 m for 3400-m thick ice. Bed topography (Figure 2a) was calculated from surface topography and ice-thickness.

[4] We used high-frequency radar to track continuous internal layers and spatially extrapolate the depth-age relationship from a 105-m core (ITASE 00-1) collected near the divide [*Neumann et al.*, 2008]. The depth-age relationship extends back to AD 1651 [*Dixon et al.*, 2004]; the ice-equivalent accumulation rate at the core site (averaged over the 349 years between AD 1651 and 2000) is 0.25 m a^{-1}. Accumulation increases almost linearly across the divide (Figure 2c); our radar-derived accumulation at WDC (0.22 m a^{-1} of ice equivalent) compares well with measurements of 0.22 and 0.23 m a^{-1} from two 130-m cores extracted in the vicinity of WDC [*Banta et al.*, 2008].

3. Mass Continuity

[5] Direct measurements of the rate of ice-thickness change $\dot{h}$ from repeat surveys of surface elevation are hampered by the need to adjust for near-surface snow density variations, and inter-annual variations in accumulation [*Helsen et al.*, 2008]. To get around this problem, we calculate $\dot{h}$ from continuity

$$\dot{h} = \dot{b} - \nabla \cdot \vec{Q} = \dot{b} - \left(\frac{\partial q_x}{\partial x} + \frac{\partial q_y}{dy} \right) \quad (1)$$

[1]Department of Earth and Space Sciences, University of Washington, Seattle, Washington, USA.

0094-8276/09/2009GL038072$05.00

where $\dot{b}$ is the ice-equivalent surface mass balance (accumulation – ablation) and $\nabla \cdot \vec{Q}$ is the horizontal flux divergence of ice.

4. Ice Flux $\vec{Q}$ and Flux Divergence $\nabla \cdot \vec{Q}$

[6] The ice flux $\vec{Q}$ has components q_x and q_y in the x and y directions:

$$\begin{pmatrix} q_x(x,y) \\ q_y(x,y) \end{pmatrix} = h(x,y)\gamma(x,y)\begin{pmatrix} u(x,y) \\ v(x,y) \end{pmatrix} \quad (2)$$

where $h(x,y)$ is the measured ice thickness and the dimensionless factor $\gamma(x, y)$ scales the components of the measured horizontal surface velocity $u(x, y)$ and $v(x, y)$ to depth-averaged velocities. The flow law for ice constrains values of $\gamma(x, y)$ to range from 0.7 at ice divides in steady state and frozen to the bed [*Schott-Hvidberg*, 1996], to 1.0 for ice sliding at the bed [*Paterson*, 1994]. Here we assume $\gamma(x, y)$ varies as a function of distance from the divide and calculate $\vec{Q}$ for three different γ-distributions. Our preferred γ-distribution (case I in Figure 2d) is based on results from *Neumann et al.* [2008] that indicate (1) the location of the Western Divide has not been stable but rather has moved around for at least 5000 years and (2) the bed is likely frozen on the Amundsen Sea side of the divide but possibly melting (and sliding) on the Ross Sea side.

[7] Assuming that variations in the ice flux are smooth within ±40 km of the divide, we fit the 98 point measurements of $\vec{Q}$ with a vector polynomial of degree P in x, y

$$\begin{pmatrix} q_x^*(x,y) \\ q_y^*(x,y) \end{pmatrix} = \sum_{k=0}^{P}\sum_{i=0}^{k}\begin{pmatrix} \alpha_{i,k-i} \\ \beta_{i,k-i} \end{pmatrix} x^i y^{k-i} \quad (3)$$

Here q_x^* and q_y^* are components of the vector polynomial $\vec{Q}^*$ that is fit to the observed vectors $\vec{Q}$. The polynomial $\vec{Q}^*$ is redundant (it is defined in line above) and could be removed to improve readability, which minimizes the mismatch to observations, is constrained so that the divergence $\nabla \cdot \vec{Q}^*$ is of degree D, and the curl $\nabla \times \vec{Q}^*$ is of degree C. The degree of the divergence is held at D by imposing the linear constraint $(i + 1)\alpha_{i+1,k-1} + (k + 1 - i)\,\beta_{i,k+1-i} = 0$, for all $k > D$ and $i \leq k$. The degree of the curl is held at C by the constraint $(i + 1)\beta_{i+1,k-1} + (k + 1 - i)\alpha_{i,k+1-i} = 0$, for all $k > C$ and $i \leq k$.

[8] All 30 polynomials for $1 \leq P \leq 4$ with $0 \leq D < P$ and $0 \leq C < P$ were considered, and each was evaluated using the statistical F-test [*von Storch and Zwiers*, 1999]. The best fit using our preferred γ-distribution ($r^2_{\vec{Q}} = 0.996$), is polynomial $P, D, C = 3, 1, 1$; that is, a 3rd degree polynomial with both the divergence and the curl varying linearly in x, y. The flux divergence $\nabla \cdot \vec{Q}^* = \frac{\partial q_x^*}{\partial x} + \frac{\partial q_y^*}{dy}$ is calculated by differentiating $\vec{Q}^*$.

5. Ice-Thickness Change

[9] Figure 3a shows the spatial pattern of ice-thickness change $\dot{h}$, calculated from equation (1) using $\nabla \cdot \vec{Q}^*$ and the radar-derived annual accumulation $\dot{b}$; Table 1 gives statistics for the five points indicated in Figure 2. Uncertainty in the divergence $\varepsilon_{\nabla \cdot \vec{Q}}$ includes uncertainties in γ, u, v and h, as well as uncertainty in the polynomial fit (Appendix A and Table 2). Uncertainty in the annual accumulation $\varepsilon_{\dot{b}}$ is taken to be 15% of $\dot{b}$ [*Banta et al.*, 2008]. Uncertainty in ice-thickness change $\varepsilon_{\dot{h}}$ is estimated by assuming that $\varepsilon_{\dot{b}}$ and $\varepsilon_{\nabla \cdot \vec{Q}}$ are uncorrelated. Most of the uncertainty in $\dot{h}$ comes from uncertainty in $\dot{b}$ (Table 1).

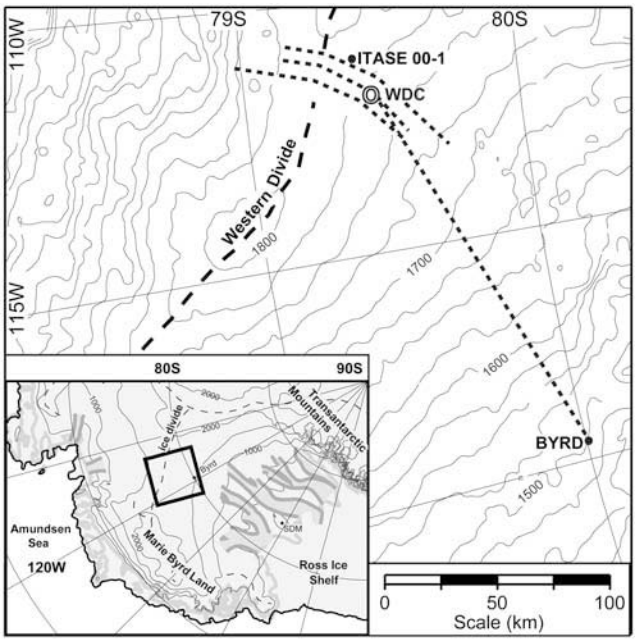

Figure 1. Surface elevations (meters above WGS 84) in the vicinity of the Western Divide between the Ross and Amundsen seas [from *Morse et al.*, 2002]. Radar-detected layers and ice thickness were tracked from dated cores at Byrd (80.017S, 119.517W) and ITASE 00-1 (79.383S, 111.229W). Primary radar lines are indicated by dashed lines; cross-profile transects are not shown. Drilling of the WAIS divide core (WDC-79.468 S, 112.086 W) started in 2007.

[10] Results indicate strong thinning ($\dot{h} = -0.11 \pm 0.05$ m a^{-1}) 10 km from the divide on the Amundsen Sea side, thinning at the divide ($\dot{h} = -0.08 \pm 0.04$ m a^{-1}), no significant thickness change at WDC, and thickening ($\dot{h} = +0.09 \pm 0.03$ m a^{-1}) 40 km from the divide on the Ross Sea side (Table 1 and Figure 3a). Our results are consistent with those detected by satellite radar altimetry that reveal strong surface lowering in the Amundsen Sea sector and slight thickening in the Ross Sea sector over the period 1995–2003 [*Helsen et al.*, 2008].

6. Discussion

[11] The observed pattern of thickness change will cause the divide to migrate toward the Ross Sea at ~10 m a^{-1}; if the pattern persists, the divide will migrate ~1 km in 100 years (Figure 3b). Divide migration is consistent with the radar-detected internal stratigraphy. At ice divides in steady state and frozen at the bed, vertical velocity at mid-depths is lower than on the flanks and hence radar-detected layers beneath the divide are arched upward [*Raymond*, 1983]. Such a distinctive stack of layering is not evident beneath the Western Divide [*Neumann et al.*, 2008]; either the bed is not frozen and/or the divide has been moving. Asymmetric thinning and migration of the Western Divide

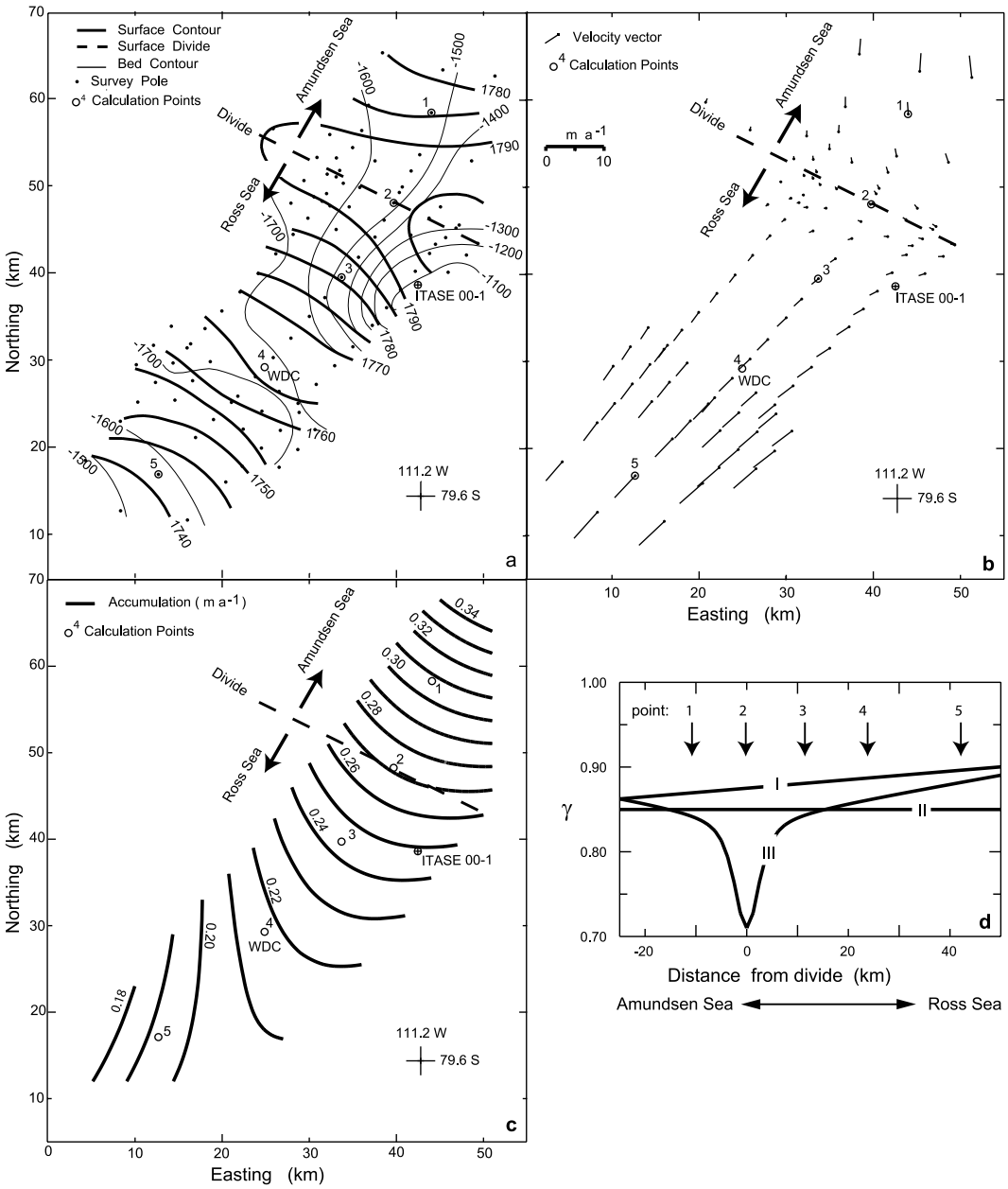

Figure 2. Survey poles across the Western Divide were set and surveyed in 2002–2003 and resurveyed in 2003–2004. (a) Measurements were used to map surface topography. Ice-penetrating radar profiles between the survey poles were used to measure ice thickness; bed topography (Figure 1a) was calculated from surface topography and ice thickness. (b) Surface velocities were calculated from the repeat surveys of pole positions; the line emanates from each pole in the direction of flow. (c) The spatial pattern of accumulation was mapped by extrapolating the depth-age relationship from ITASE 00-1 using near-surface radar-detected layers. (d) The γ-distributions used to scale observed surface velocities to depth-averaged velocities. Case III is for a divide that is in steady state and frozen to the bed [*Schott-Hvidberg*, 1996]. Case II is for constant $\gamma = 0.85$. Case I is our preferred distribution, which is based on results from *Neumann et al.* [2008]. Points 1–5 are used for calculations shown in Table 1; points 1–3 and 5 coincide with locations of survey poles.

have consequences for interpretation of the WAIS divide ice core located on the Ross Sea side of the divide. Particle paths may be complex; it is possible that some of the deeper ice now at the core site originated from the Amundsen Sea side of the present divide.

[12] Although the accumulation rate 3000 years ago was about 30% higher than present, its gradient across the divide has not changed for at least 5000 years [*Neumann et al.*, 2008]; the pattern of thickness change is a result of asymmetric dynamical thinning on either side of the divide rather than changes in the accumulation-rate gradient.

[13] The characteristic timescale for ice sheets is the ratio of ice-thickness to the accumulation rate $h/\dot{b}$ [*Paterson*, 1994]; for the Western Divide (h = 3400 m and $\dot{b}$ = 0.27 m a^{-1}), $h/\dot{b}$ = 12,000 years. However, the relaxation time for adjustment of divide position to a perturbation at the margin is a small fraction of $h/\dot{b}$ [*Hindmarsh*,

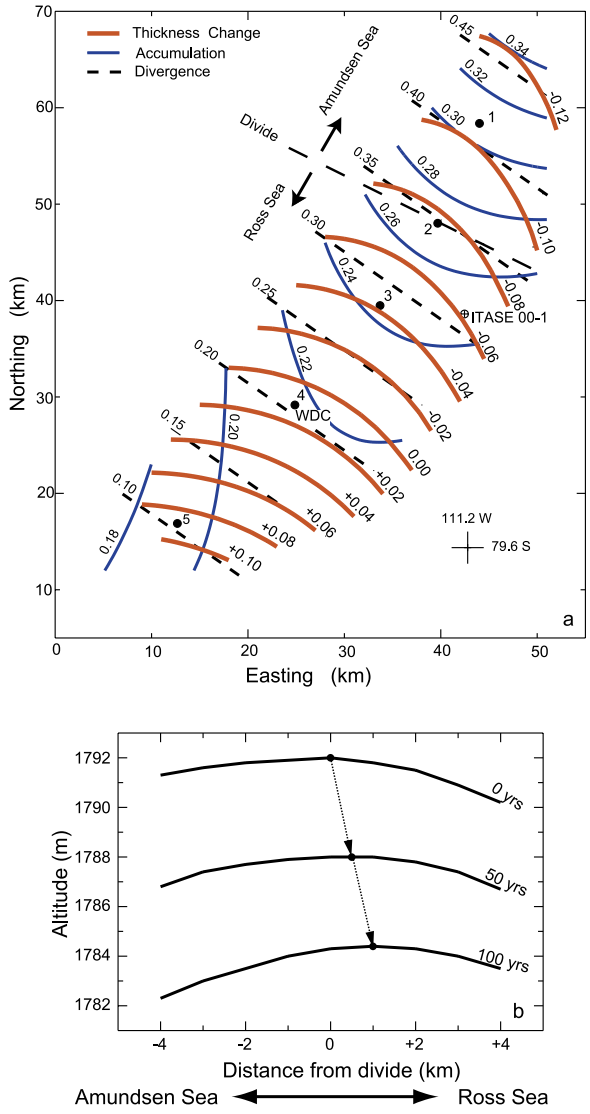

Figure 3. (a) Flux divergence $\nabla \cdot \vec{Q}^*$ calculated using the best fitting polynomial and our preferred γ-distribution, radar-derived accumulation $\dot{b}$, and the rate of ice-thickness change calculated from the difference between $\dot{b}$ and $\nabla \cdot \vec{Q}^*$. (b) Thinning and migration of the divide that would occur if the present-day pattern of thickness change persists for 50 and for 100 years.

1996]; the relaxation time for the Western Divide is expected to be about 1000 years and the corresponding volumetric response time is about twice that [*Nereson et al.*, 1998]. Theory that the Western Divide is now responding to perturbations over millennial timescales is consistent with evidence from exposure ages from rock outcrops in the Amundsen Sea sector that indicate thinning has been ongoing there for at least 4500 years [*Johnson et al.*, 2008], while exposure ages from the Ross Sea sector indicate that grounding-line retreat and thinning there stopped 2000–3000 years ago (J. O. Stone et al., Grounding-line retreat into the southernmost Ross Sea: A comparison between lower Scott and Reedy Glaciers, paper presented at 12th Annual West Antarctic Ice Sheet Workshop, Sterling, Va., 2005).

[14] It is also possible the divide is responding to more recent dynamical changes. The onset of fast flow of a tributary of Thwaites Glacier is within 70 km of the divide [*Joughin et al.*, 2009], while those of tributaries of Kamb and Bindschadler Ice Streams in the Ross Sea sector are within 100 km of it. This configuration allows perturbations at the grounding line to be transmitted to within 100 km of the divide over decadal timescales [e.g., *Payne et al.*, 2004]; in this case the divide could be responding to centennial rather than millennial forcing. Following this hypothesis, the mass gain in the Ross Sea sector since the slow down of Kamb Ice Stream about two centuries ago [*Joughin and Tulaczyk*, 2002], and the mass loss in the Amundsen Sea sector over the past few decades [*Rignot et al.*, 2008], could also be contributing to the present-day divide migration.

[15] Our data, however, are not sufficient to determine whether the Western Divide is responding to long-term (millennial) forcing, shorter-term (centennial) forcing, or both. Continued monitoring of the pattern of ice-thickness change and the rate of divide migration would help establish the dynamic coupling between coastal regions and the divide. It may also be possible to resolve the history of ice-thickness

Table 2. Sensitivity of $\nabla \cdot \vec{Q}^*$ to Assumptions[a]

	Polynomial				$\nabla \cdot \vec{Q}^*$ (m yr^{-1})				
Case	P	D	C	$\gamma(x, y)$	1	2	3	4	5
1	3	1	1	I	0.415	0.347	0.285	0.205	0.104
2	4	1	1	I	0.404	0.340	0.280	0.201	0.097
3	4	1	2	I	0.405	0.341	0.281	0.204	0.098
4	3	2	1	I	0.403	0.337	0.278	0.201	0.106
5	3	1	2	I	0.411	0.346	0.286	0.208	0.109
6	3	1	1	II	0.413	0.341	0.275	0.191	0.085
7	3	1	1	III	0.396	0.334	0.278	0.206	0.115
8					0.006	0.004	0.004	0.005	0.009
9					0.009	0.006	0.006	0.004	0.006
10					0.011	0.008	0.007	0.007	0.011

[a]Results are for the five points shown in Figure 2. Cases 1–5 are statistically best fit polynomials in decreasing F-test order. Distributions $\gamma(x, y)$ are shown in Figure 2d. Case 8 is standard deviation of cases 1–7; case 9 is ε_{∇} (calculated from equation (A2)); case 10 is $\varepsilon_{\nabla \cdot Q}$, the resultant of cases 8 and 9, assuming that they are independent sources of error.

Table 1. Statistics for the Five Calculation Points Shown in Figure 2[a]

	1	2	3	4	5
$\nabla \cdot \vec{Q}^*$ (m yr^{-1})	0.415 ± 0.011	0.347 ± 0.008	0.285 ± 0.007	0.205 ± 0.007	0.104 ± 0.011
$\dot{b}$ (m yr^{-1})	0.310 ± 0.047	0.270 ± 0.041	0.242 ± 0.036	0.217 ± 0.033	0.192 ± 0.029
$\dot{h}$ (m yr^{-1})	−0.105 ± 0.048	−0.077 ± 0.042	−0.043 ± 0.037	+0.012 ± 0.034	+0.088 ± 0.031

[a]Flux divergence $\nabla \cdot \vec{Q}^*$ calculated using the best fitting polynomial with our preferred γ-distribution, radar-derived ice-equivalent accumulation $\dot{b}$, and the rate of ice-thickness change $\dot{h}$ calculated from equation (1). Uncertainty in the flux divergence ε_{∇} includes uncertainties in γ, u, v, and h, as well as in the polynomial fit (Table 2). Uncertainty in annual accumulation $\varepsilon_{\dot{b}}$ is assumed to be 15% of $\dot{b}$. Uncertainty in ice-thickness change is calculated assuming $\varepsilon_{\dot{b}}$ and ε_{∇} are uncorrelated.

change across the divide by using dated radar-detected internal layers to constrain a transient ice-flow model M. Koutnik et al., manuscript in preparation, 2009).

Appendix A: Analysis of Uncertainties

[16] Given uncertainties ε_h in h, ε_γ in γ, as well as ε_u and ε_v in the components of the surface velocity, uncertainty in the components q_x and q_y of the flux vector $\vec{Q}$ (ε_x and ε_y) comes from application of the algebra of error propagation [*Bevington*, 1969]:

$$\begin{pmatrix} \varepsilon_x^2 \\ \varepsilon_y^2 \end{pmatrix} = \left(h^2\varepsilon_\gamma^2 + \gamma^2\varepsilon_h^2\right)\begin{pmatrix} u^2 \\ v^2 \end{pmatrix} + \gamma^2 h^2 \begin{pmatrix} \varepsilon_u^2 \\ \varepsilon_v^2 \end{pmatrix}.$$

Mismatch between the vector polynomial and the observed $\vec{Q}$ over the $N_Q = 98$ observations is $E = rms_x^2 + rms_y^2 = \frac{1}{N_Q}\sum^{N_Q}\left(\frac{q_x^* - q_x}{\varepsilon_x}\right)^2 + \frac{1}{N_Q}\sum^{N_Q}\left(\frac{q_y^* - q_y}{\varepsilon_y}\right)^2$. Goodness of fit is $r_x^2 = 1 - \left[\frac{rms_x}{\sigma_x}\right]^2$, $r_y^2 = 1 - \left[\frac{rms_y}{\sigma_y}\right]^2$, and $r_Q^2 = 1 - \frac{rms_x^2 + rms_y^2}{\sigma_x^2 + \sigma_y^2}$ overall, in which $\sigma_x = 3.63$ m-km a^{-1} and $\sigma_y = 4.96$ m-km a^{-1} are the standard deviations of the observed q_x and q_y.

[17] The flux divergence is

$$\begin{aligned} \nabla \cdot \vec{Q} &= \frac{\partial q_x}{\partial x} + \frac{\partial q_y}{dy} \\ &= \gamma u \frac{\partial h}{\partial x} + hu\frac{\partial \gamma}{\partial x} + h\gamma\frac{\partial u}{\partial x} + \gamma v\frac{\partial h}{\partial y} + hv\frac{\partial \gamma}{\partial y} + h\gamma\frac{\partial v}{\partial y} \end{aligned} \quad \text{(A1)}$$

Assuming that uncertainties in γ, u, v and h are uncorrelated with each other, uncertainty in the flux divergence at any point is

$$\begin{aligned} \varepsilon_\nabla^2 = {} & \varepsilon_\gamma^2\left[u^2\left(\frac{\partial h}{\partial x}\right)^2 + h^2\left(\frac{\partial u}{\partial x}\right)^2 + v^2\left(\frac{\partial h}{\partial y}\right)^2 + h^2\left(\frac{\partial v}{\partial y}\right)^2\right] \\ & + \varepsilon_h^2\left[u^2\left(\frac{\partial \gamma}{\partial x}\right)^2 + \gamma^2\left(\frac{\partial u}{\partial x}\right)^2 + v^2\left(\frac{\partial \gamma}{\partial y}\right)^2 + \gamma^2\left(\frac{\partial v}{\partial y}\right)^2\right] \\ & + \varepsilon_u^2\left[\gamma^2\left(\frac{\partial h}{\partial x}\right)^2 + h^2\left(\frac{\partial \gamma}{\partial x}\right)^2\right] + \varepsilon_v^2\left[\gamma^2\left(\frac{\partial h}{\partial y}\right)^2 + h^2\left(\frac{\partial \gamma}{\partial y}\right)^2\right] \end{aligned} \quad \text{(A2)}$$

To avoid differentiating the surface velocity field itself, the derivatives $\partial u/\partial x$ and $\partial v/\partial y$ are determined from $\frac{\partial u}{\partial x} = \frac{1}{h\gamma}\frac{\partial q_x}{\partial x} - \frac{u}{h}\frac{\partial h}{\partial x} - \frac{u}{\gamma}\frac{\partial \gamma}{\partial x}$ and $\frac{\partial v}{\partial y} = \frac{1}{h\gamma}\frac{\partial q_y}{\partial y} - \frac{v}{h}\frac{\partial h}{\partial y} - \frac{v}{\gamma}\frac{\partial \gamma}{\partial y}$. Values adopted here are $\varepsilon_h = 42$ m, $\varepsilon_\gamma = 0.01$, and $\varepsilon_u = \varepsilon_v = 0.04$ m a^{-1}. Table 2 summarizes statistics for the five points shown in Figure 2. Cases 1–5 are for the five best fitting polynomials, with our preferred γ-distribution, in decreasing F-test order. Results in cases 6 and 7 are for different γ-distributions. Case 8 is the standard deviation of cases 1–7.

[18] **Acknowledgments.** US National Science Foundation (OPP-0087345 and OPP-0440666) funded this work. We also thank G. Catania, M. Conway, K. Matsuoka, D. L. Morse, T. A. Neumann, F. Ng, E. Pettit, D. Power, S. F. Price, and E. D. Waddington for assistance in the field and GPS data processing; UNAVCO for GPS support; and Raytheon Polar Services, Air National Guard, and Kenn Borek Air for logistical support. Comments and discussions with R. B. Alley, B. L. Hall, I. Joughin, E. Rignot, C. F. Raymond and E. D. Waddington and an anonymous reviewer improved the paper.

References

Alley, R. B., D. D. Blankenship, C. R. Bentley, and S. T. Rooney (1987), Till beneath Ice Stream B:4. A coupled ice-till flow model, *J. Geophys. Res.*, *92*, 8931–8940.

Banta, J. R., J. R. McConnell, M. M. Frey, R. C. Bales, and K. Taylor (2008), Spatial and temporal variability in snow accumulation at WAIS Divide over recent centuries, *J. Geophys. Res.*, *113*, D23102, doi:10.1029/2008JD010235.

Bevington, P. R. (1969), *Data Reduction and Error Analysis for the Physical Sciences*, McGraw-Hill, New York.

Dixon, D., P. A. Mayewski, S. Kaspari, S. Sneed, and M. Handley (2004), A 200-year sub-annual record of sulfate in West Antarctica from 16 ice cores, *Ann. Glaciol.*, *39*, 545–556.

Helsen, M. M., et al. (2008), Elevation changes in Antarctica mainly determined by accumulation variability, *Science*, *320*, 1626–1629.

Hindmarsh, R. C. A. (1996), Stochastic perturbation of divide position, *Ann. Glaciol.*, *23*, 94–104.

Johnson, J. S., M. J. Bentley, and K. Gohl (2008), First exposure ages from the Amundsen Sea Embayment, West Antarctica: The late Quaternary context for recent thinning of Pine Island, Smith, and Pope Glaciers, *Geology*, *36*, 223–226, doi:10.1130/G24207A.1.

Joughin, I., and S. Tulaczyk (2002), Positive mass balance of the Ross Ice Streams, West Antarctica, *Science*, *295*, 476–480.

Joughin, I., S. Tulaczyk, J. L. Bamber, D. Blankenship, J. W. Holt, T. Scambos, and D. G. Vaughan (2009), Basal conditions for Pine Island and Thwaites Glaciers determined using satellite and airborne data, *J. Glaciol.*, *55*, 245–257.

Morse, D. L., D. D. Blankenship, E. D. Waddington, and T. A. Neumann (2002), A site for deep ice coring in West Antarctica: Results from aerogeophysical surveys and thermo-kinematic modeling, *Ann. Glaciol.*, *35*, 36–44.

Nereson, N. A., R. C. A. Hindmarsh, and C. F. Raymond (1998), Sensitivity of the divide position at Siple Dome to boundary forcing, *Ann. Glaciol.*, *27*, 207–214.

Neumann, T. A., H. Conway, S. F. Price, E. D. Waddington, G. A. Catania, and D. L. Morse (2008), Holocene accumulation and ice sheet dynamics in central West Antarctica, *J. Geophys. Res.*, *113*, F02018, doi:10.1029/2007JF000764.

Paterson, W. S. B. (1994), *The Physics of Glaciers*, 3rd ed., Pergamon, Oxford, U. K.

Payne, A. J., A. Vieli, A. P. Shepherd, D. J. Wingham, and E. Rignot (2004), Recent dramatic thinning of largest West Antarctic ice stream triggered by oceans, *Geophys. Res. Lett.*, *31*, L23401, doi:10.1029/2004GL021284.

Raymond, C. F. (1983), Deformation in the vicinity of ice divides, *J. Glaciol.*, *29*, 357–373.

Rignot, E., et al. (2008), Recent Antarctic ice mass loss from radar interferometry and regional climate modelling, *Nat. Geosci.*, *1*, 106–110.

Schott-Hvidberg, C. (1996), Steady-state thermo-mechanical modelling of ice flow near the center of large ice sheets with finite-element technique, *Ann. Glaciol.*, *23*, 116–123.

Shepherd, A., D. J. Wingham, and E. Rignot (2004), Warm ocean is eroding West Antarctic Ice Sheet, *Geophys. Res. Lett.*, *31*, L23402, doi:10.1029/2004GL021106.

von Storch, H., and F. W. Zwiers (1999), *Statistical Analysis in Climate Research*, Cambridge Univ. Press, New York.

H. Conway and L. A. Rasmussen, Department of Earth and Space Sciences, University of Washington, Seattle, WA 98195, USA. (conway@ess.washington.edu)